IL-23 producing IL-10Rα-deficient gut macrophages elicit an IL-22-driven pro-inflammatory epithelial cell response

Biana Bernshtein[1], **Caterina Curato**[1], **Marianna Ioannou**[3], **Christoph A Thaiss**[1], **Mor Gross-Vered**[1], **Masha Kolesnikov**[1], **Qian Wang**[2], **Eyal David**[1], **Louise Chappell-Maor**[1], **Alon Harmelin**[3], **Eran Elinav**[1], **Paresh Thakker**[4], **Venizelos Papayannopoulos**[2], **Steffen Jung**[1,†]

[1]Department of Immunology, Weizmann Institute of Science, Rehovot 76100, Israel

[2]The Francis Crick Institute, London NW1 1AT

[3]Department of Veterinary Resources, Weizmann Institute of Science, Rehovot 76100, Israel

[4]Boehringer Ingelheim Pharmaceuticals Inc., Ridgefield, CT

Abstract

Several cytokines maintain intestinal health, but precise inter-cellular communication networks remain poorly understood. Macrophages are immune sentinels of the intestinal tissue, critical for gut homeostasis. Here we show that in a murine IBD model based on macrophage-restricted Interleukin 10 (IL-10) receptor deficiency (*Cx3cr1^{Cre}:Il10ra^{fl/fl}* mice), pro-inflammatory mutant gut macrophages cause severe spontaneous colitis resembling the condition of children carrying IL10R mutations. We establish macrophage-derived IL-23 as the driving factor of this pathology. Specifically, we report that *Cx3cr1^{Cre}: Il10ra^{fl/fl}:Il23a^{fl/fl}* mice harboring macrophages deficient for both IL-10R and IL-23 are protected from colitis. By analyzing the epithelial response to pro-inflammatory macrophages, we provide evidence that T cells of colitic animals produce deleterious IL-22 that induces epithelial chemokine expression and detrimental neutrophil recruitment. Collectively, we define critical cell-type-specific contributions to the induction and effector mechanism of macrophage-driven colitis, as manifested in mice harboring IL-10R deficiencies and human IBD pathologies.

Introduction

Inflammatory bowel disorders (IBD) comprise with Crohn's disease (CD) and ulcerative colitis (UC) two chronic and relapsing pathologies of the small and large intestine that affect millions of individuals world-wide (1). Extensive genome wide association studies (GWAS)

revealed 200 IBD-associated genetic loci and recent high-resolution fine-mapping identified statistically convincing causal variants (2). In parallel, studies in mice have yielded unprecedented understanding of the cellular composition of the intestinal mucosa, including mononuclear phagocytes (3), adaptive and innate lymphoid cells (ILC) (4), inter-cellular communication circuits maintaining gut homeostasis (5), as well as the impact of microbiota (6). Animal IBD models have provided critical mechanistic insights to define genetic factors causing, contributing to or preventing intestinal inflammation (7). One such module consists of the cytokine Interleukin 10 (IL-10), its specific receptor IL-10R (9, 10), and associated signaling components, such as Stat3 (8, 9).

Most intestinal macrophages reside in the connective tissue or *lamina propria*, underlying the monolayer of epithelial cells (EC). As non-migratory cells, they do not translocate to draining lymph nodes and display limited or no potential to 'prime' naive T cells (10). In adult mice, most *lamina propria* macrophages are continuously replenished by Ly6C^{hi} blood monocytes (11, 12). Monocyte-derived cells replace an embryonically derived population in the gut shortly after birth (13). As opposed to many other tissue macrophages that efficiently self-renew in their entirety throughout adult life (10), adult intestinal macrophages comprise subsets with distinct half-lives (14). Constant replacement of short-lived gut macrophages necessitates ongoing adaption of monocyte precursors to the dynamic local gut environment, including the prominent exposure to microbial stimuli (15). IL-10, provided by T regulatory cells (16), is a critical factor ensuring colon homeostasis and preventing the emergence of proinflammatory monocyte-derived cells. Specifically, colonic macrophages unable to sense IL-10 due to a *Il-10ra* deficiency fail to be restrained in patients (17, 18). Moreover, also mice harboring Il10Ra-deficient macrophages develop severe early onset colitis (19), and hence provide a valuable model for mechanistic studies of the human disorder caused by the *Il-10ra* loss-of-function mutation.

IL-10 receptor-deficient macrophages display a pro-inflammatory expression signature, including up-regulation of IL-23 (19), a cytokine composed of two subunits: p19 which is unique to IL-23; and p40 which is shared with IL-12 (20). IL-23 was shown to contribute to colitis development in several mouse models. Following *Helicobacter hepaticus (Hh)* infection of lymphopenic *Rag2*^{-/-} mice, antibody-mediated neutralization of p19 or p40, but not p35 (the second IL-12 subunit) ameliorated disease (21). Likewise, *Il23a*^{-/-}:*Rag1*^{-/-} and *Il12b*^{-/-}:*Rag1*^{-/-}, but not *Il12a*^{-/-}:*Rag1*^{-/-} mice are protected from T cell transfer-induced colitis (21). Moreover, following a combination of *Hh* infection and IL-10R blockade, wild type (WT) and *Il12a*^{-/-} mice succumb to disease, whereas *Il12b*^{-/-} mice are spared (22). As for the mechanism by which IL-23 drives inflammation, involvement of IFNγ-secreting Th1 cells and reduced IL-17 levels were proposed, although differentiation of Th17 cells was unaltered in absence of IL-23 (21). Supporting IL-23 action on T cells, adoptive transfers of IL-3R-deficient T cells into immuno-deficient mice cause less severe colitis than WT T cell engraftment (23). Several cell types were suggested as the source of IL-23, including monocytes, Cx3cr1^{+} macrophages and CD103^{+} CD11b^{+} dendritic cells, while their respective contributions might differ in the small and large intestine (24–27).

T cell responses to IL-23 include production of IL-22, a cytokine acting on EC and in colitis context widely considered anti-inflammatory. Thus, IL-22 therapy by gene transfer and

IL-22–producing neutrophils were shown to ameliorate colitis (28). Likewise, IL-22-deficient mice display increased gut inflammation, both in the DSS and the T-cell transfer colitis model (29). In contrast, in dermal inflammatory diseases, such as psoriasis, IL-22 was shown to play a detrimental role (30). Pro-inflammatory activities of IL-22 in the gut were reported for an innate-driven colitis model based on the injection of anti-CD40 antibody, which stimulates myeloid cells (31)and causes dysbiosis favoring pathogen colonization potentially due to IL-22-induced antimicrobial peptide (AMP) production (31). Collectively, IL-22 is widely considered a beneficial agent in gut inflammation, and described to be involved in wound healing and bacterial protection (32–34). Accordingly, IL-22 therapy has been suggested as a possible treatment for IBD patients (30), disregarding possible deleterious outcome of chronic IL-22 stimulation of gut EC.

Here we investigated macrophage-driven colitis, as manifested in children and mice harboring IL-10R deficiencies (17, 18, 35). Specifically, we define causative cell responses and reveal the critical role of the IL-23 / IL-22 pathway in this IBD pathology. We report that pro-inflammatory macrophages produce IL-23, which in turn recruits Th17 cells and induces secretion of IL-22. Colonic EC respond to IL-22 exposure by expression of AMP and neutrophil chemoattractants that seem critical for colitis development.

Results

IL10Ra-deficient macrophages confer spontaneous colitis involving the IL-23 / IL-22 axis

In mice and human, intestinal macrophages require IL-10 sensing to maintain gut homeostasis (17–19). Accordingly, $Cx3cr1^{cre}:Il10ra^{fl/fl}$ mice harbouring IL-10Ra-deficient macrophages develop spontaneous colitis manifested in IBD hallmarks, including tissue remodelling and immune cell infiltrates in the colon, but not the ileum (19).

Intestinal macrophages extracted from colonic *lamina propria* of 6-7 weeks old pre-colitic $Cx3cr1^{cre}:Il10ra^{fl/fl}$ mice displayed a pro-inflammatory gene expression signature (Fig 1a, b, Supp Fig1). Mutant macrophages exhibit elevated expression of cytokine and chemokine genes, including *il23a*, *il12b*, *ccl5*, genes encoding activation markers such as *trem1*, and inflammatory molecules, like *nos2* and *saa3*. In total, 310 genes were significantly down-regulated and 355 genes were significantly up-regulated in mutant cells, as compared to controls (fold change >2, adjusted p-value <0.05).

IL-23R was identified by GWAS as an IBD susceptibility gene (36), and IL-23-deficient mice are resistant to colitis induction in different IBD mouse models (21, 22, 37). IL-10ra-deficient macrophages expressed high levels of *Il23a*, as revealed by RNAseq (Fig 1B) and confirmed by qRT-PCR conducted on sorted colonic macrophages (Fig 1C). Antibiotic treatment upon weaning abolished the proinflammatory signature of IL10Ra-deficient colonic macrophages (Supp Fig 1B) and IL-23 up-regulation (Fig 1C), establishing microbiota-derived signals as macrophage activation stimuli in this model. IL-23 is known to induce IL-22 expression by Th17 cells and type 3 innate lymphoid cells (ILC3) (38, 39). Accordingly, *Il22* mRNA levels were elevated in the tissue of mice harbouring IL-10Ra deficient macrophages in a microbiota-dependent manner (Fig 1C). Additionally, and in line with possible involvement of Th17 cells in this colitis model, IL-17 transcript levels were

significantly up-regulated in whole tissue extracts of colitic mice (Fig 1D). Differential contributions of Th17 cells and ILC3 to colitis development remain controversial (4). To study their role in the present colitis model, we crossed *Cx3cr1*^{cre}*:Il10ra*$^{fl/fl}$ animals to *Rorgt*^{gfp} reporter mice (40), allowing identification and discrimination of ILC3 and Th17 cells by flow cytometry and histology (Fig 1E, F). The *lamina propria* of colitic *Cx3cr1*^{cre}*:Il10ra*$^{fl/fl}$*:Rorgt*^{gfp} animals was abundantly populated with ILC3 and Th17 cells (Fig 1E, F; Supp Fig 1C), both of which expressed elevated *Il22* mRNA levels as compared to cells isolated from *Il10ra*$^{fl/fl}$*:Rorgt*^{gfp} control littermates (Fig 1G, H). ILC3 extracted from colitic mice also expressed elevated levels of *Cxcr6*, a chemokine receptor critical for the localization and IL-22 production in the small intestine (41) (Fig 1H).

Collectively, *Cx3cr1*^{cre}*:Il10ra*$^{fl/fl}$ mice display a microbiota-dependent activation of the IL-23 / IL-22 axis. Pro-inflammatory intestinal macrophages that lack IL-10R produce IL-23, and promote the accumulation and IL-22 production of both Th17 cells and ILC3.

Epithelial cells respond to pro-inflammatory macrophages by induction of IL22-dependent genes

Cx3cr1^{cre}*:Il10ra*$^{fl/fl}$ bone marrow (BM) transplants into lethally irradiated WT recipients induced spontaneous colitis, evident within 6-7 weeks following engraftment. Specifically, mice that received the colitogenic BM, but not recipients of *Cx3cr1*$^{gfp/+}$ control BM, displayed attenuated weight gain and high colonoscopy scores 7 weeks post-transplant (Fig 2A). The main IL-22 sensors in the colon are EC (4). To determine the epithelial response to IL10Ra-deficient macrophages, we implemented a reporter-based system, avoiding contaminations by immune cells, which reside in the epithelial layer. Specifically, we took advantage of *Villin*^{cre}*:R26-tdTomato* mice (42), whose colonic and ileal EC, but not CD45$^+$ cells, express a tomato reporter protein detectable by histology and flow cytometry (Fig 2B, C). Of note, colonic EC extracted from irradiated mice showed few differentially expressed genes as compared to EC isolated from non-irradiated animals (Supp Fig 2 A, C), and hence do not display persistent transcriptomic changes in agreement with their reported efficiency to cope with irradiation damage (43).

Colitogenic *Cx3cr1*^{cre}*:Il10ra*$^{fl/fl}$ BM was grafted into irradiated *Villin*^{cre}*:R26-tdTomato* recipients and Tomato$^+$ colonic and ileal EC were isolated at two time points, *i.e.* prior to overt disease onset (14 days post-transplant (dpt)) and upon signs of colonic inflammation (60 dpt) (Fig 2D). RNAseq analysis revealed significant transcriptomic changes of colonic EC at 14 dpt, which increased 60 dpt, with 316 and 834 differentially expressed genes, respectively (Fig 2E). In contrast to the colonic EC, ileal EC showed minimal changes at both time points, even though they had been isolated from the same animal (Supp Fig 2B). Differentially expressed genes of colonic EC at early and late time points comprised a prominent signature of IL-22-induced genes (4), including AMP, CXC chemokines and members of the calcium binding S100 protein family (*S100a8, S100a9*) that encode calprotectin (Fig 2F). The chemokines and S100 were absent from ileal EC transcriptomes (Fig 2F). The two subunits comprising the IL22 receptor, *Il10rb* and *Il22ra,* were expressed by both ileal and colonic EC under steady state and inflammatory conditions (Supp Fig 2D), indicating the ability of EC to sense IL22 in both ileum and colon under steady state

conditions. Expression of the IL10 specific receptor subunit *il10ra* was below background levels. Importantly, robust AMP and chemokine up-regulation was not restricted to colitic BM chimeras, but also observed in *Cx3cr1^{cre}:Il10ra$^{fl/fl}$* mice, which displayed up-regulation of *Reg3b*, *Reg3g*, *Cxcl1* and *Cxcl5*, already at 6-7 weeks of age when signs of colitis were mild, as compared to co-housed *Il10ra$^{fl/fl}$* littermate controls (Fig 2G, Supp Fig 2F). In conclusion, prior to overt signs of intestinal inflammation colonic EC respond to pro-inflammatory macrophages, including the expression of AMP and chemokines that are established to be IL-22-induced.

Mutant macrophage production of IL-23 drives colitis in *Cx3cr1^{cre}:Il10ra$^{fl/fl}$* mice

The central role of IL-23 has been established in IBD models (21, 22, 37), but the critical cellular sources of this cytokine remain controversial and might differ between anatomic location and pathology (24–27). Moreover, in our system colonic IL-10R deficient macrophages produce other pro-inflammatory factors, including Ccl5, Nos2, Saa3 and Il12b, in addition to IL-23 (Fig 1A, B); macrophage-derived IL-23 hence is unlikely to be the sole driver of pathology. To nevertheless probe for such a scenario in this colitis model, we generated *Cx3cr1^{cre}:Il10ra$^{fl/fl}$:Il23a$^{fl/fl}$* mice (44). Strikingly, intestinal macrophages of these animals, which in addition to failing to sense IL-10 are unable to produce IL-23, lost the complete pro-inflammatory signature, including the above-mentioned pro-inflammatory factors (Fig 3A-C). Thus, *Il10ra* / *Il23* double-deficient cells displayed only seven differentially expressed genes compared to *Cx3cr1^{gfp}* control macrophages (Fig 3C); in contrast 464 genes were found differentially expressed between macrophages isolated from *Cx3cr1^{cre}:Il10ra$^{fl/fl}$* compared to the same *Cx3cr1^{gfp}* macrophages (Fig 3B).

Mere genetic neutralization of macrophage-derived IL-23 rescued *Cx3cr1^{cre}: Il10ra$^{fl/fl}$:Il23a$^{fl/fl}$* mice from colitis, as evident from colonoscopy and histopathology analysis of co-housed age matched littermates (Fig 3D, E). In absence of macrophage-derived IL-23, tissue *Il-22* expression returned to homeostatic levels, as did expression of genes coding for AMP and Nos2 (Fig 3F). Data obtained from corresponding BM chimeras corroborated the above observation (Supp Fig3). Collectively, these data establish that the critical IL-23 source driving colitis in *Cx3cr1^{cre}:Il10ra$^{fl/fl}$* mice are macrophages, *i.e.* the same cells that lack IL-10 signalling. Moreover, our results emphasize the importance of IL-23 for disease initiation and establish that directly or indirectly, this factor induces a secondary pro-inflammatory gene signature in the macrophages.

IL-22 is required for IL-23-driven colitis in *Cx3cr1^{cre}:Il10ra$^{fl/fl}$* mice

IL-23 induces intestinal ILC3, Th17 cells and neutrophils to produce IL-22 (45), which is widely considered to be beneficial (28, 29), but can under certain circumstances also be harmful (31). Given the epithelial 'IL-22 response' to IL-10Ra-deficient macrophages (Fig 2F), we tested the impact of IL-22 in our colitis model. Specifically, we crossed *Cx3cr1^{cre}:Il10ra$^{fl/fl}$* mice to *Il22$^{-/-}$* animals (39). Interestingly, *Cx3cr1^{cre}:Il10ra$^{fl/fl}$:Il-22$^{-/-}$* mice did not develop signs of colitis, as determined by colonoscopy and histopathological evaluation (Fig 4A, B). Levels of *Il22* and neutrophil-recruiting chemokines *Cxcl1* and *Cxcl5,* as well as *Reg3b*, *Reg3g* and *Nos2* in colonic tissue of *Cx3cr1^{cre}:Il10ra$^{fl/fl}$:Il22$^{-/-}$* mice were similar to those of *Il10ra$^{fl/fl}$:Il22$^{-/-}$* littermate controls (Fig 4C). Collectively, this

establishes IL-22 in the *Cx3cr1^{cre}:Il10ra$^{fl/fl}$* model as a pro-inflammatory factor that is essential for colitis induction. Of note, although the *Cx3cr1^{cre}:Il10ra$^{fl/fl}$:Il22$^{-/-}$* mice did not exhibit intestinal pathology, their colonic macrophages displayed elevated levels of *Il23a*, as compared to *Il10ra$^{fl/fl}$:Il22$^{-/-}$* littermates (Fig 4D). In contrast and supporting the notion that their induction is a secondary effect potentially requiring the EC response, *Ccl5* transcripts were not elevated in macrophages (Fig 4D). Additionally, levels of *il17a* transcripts were increased in colonic tissues of *Cx3cr1^{cre}:Il10ra$^{fl/fl}$:Il22$^{-/-}$* mice, suggesting that in our model, IL-17 alone is insufficient to induce AMP and chemoattractant expression by EC (Fig 4C, D). Finally, flow cytometry analysis by intracellular staining of colonic lamina propria T cells of *Cx3cr1^{cre}:Il10ra$^{fl/fl}$:Il22$^{-/-}$* mice and their littermates showed increased numbers of IL17 producing T cells, in the former (Fig 4E). Collectively, our data suggest that in our model IL-22 is a required factor for colitis initiation, and its induction is the critical colitogenic response to il23a produced by IL10R-deficient proinflammatory macrophages.

Unexpectedly, WT mice that received *Cx3cr1^{cre}:Il10ra$^{fl/fl}$:Il22$^{-/-}$* BM grafts succumbed to colitis like [*Cx3cr1^{cre}:Il10ra$^{fl/fl}$* > WT] BM chimeras (Fig 5A). qRT-PCR analysis of colonic tissue of colitic BM chimeras showed elevated transcripts of the neutrophil recruiting chemokines *Cxcl1* and *Cxcl5*, but also *Il22* mRNA (Fig 5B), suggesting derivation of the latter from host cells that survived the irradiation. Indeed, irradiated *Il22$^{-/-}$* recipients that received the otherwise colitogenic *Cx3cr1^{cre}:Il10ra$^{fl/fl}$:Il22$^{-/-}$* BM were devoid of *Il22* and protected from colitis, as compared to WT recipients (Fig 5C). While corroborating the notion of IL-22 as a proinflammatory factor, this suggests radio-resistant cells as a critical IL-22 source in the *Cx3cr1^{cre}:Il10ra$^{fl/fl}$* colitis model. To probe for radio-resistant Rorgt-expressing host cells, we generated BM chimeras using Rorgt^{gfp} mice as recipients. GFP$^+$ Th17 cells, but not GFP$^+$ TCR-negative ILC3, were abundantly found in the *lamina propria* of both [*Cx3cr1^{cre}:Il10ra$^{fl/fl}$* > *Rorgt^{gfp}*] and [*Il10ra$^{fl/fl}$* > *Rorgt^{gfp}*] chimeras three weeks after BM transplantation (Fig 5D). Th17 cell numbers were significantly higher in *Cx3cr1^{cre}:Il10ra$^{fl/fl}$* BM recipients (Fig 5D), and sorted Th17 cells from these colitic chimeras exhibited elevated *Il22* transcription (Fig 5E), indicating IL-23 encounter and activation. Finally, [*Cx3cr1^{cre}:Il10ra$^{fl/fl}$* > *Il22$^{-/-}$*] BM chimeras exhibited reduced colitis progression (Fig 5F) and low *Il22* and *Cxcl5* whole tissue mRNA levels. This result excludes the possibility of IL-22 production by graft-derived cells, supporting the notion of a radio-resistant cell as the exclusive IL-22 source. Collectively, these data suggest that the critical colitogenic cellular source of IL-22 in the *Cx3cr1^{cre}:Il10ra$^{fl/fl}$* colitis model are radioresistant cells, which include Th17 cells.

CD4$^+$ cells are critical for IL-22 production and neutrophil accumulation in *Cx3cr1^{cre}:Il10ra$^{fl/fl}$* colitis model

Next, we aimed to further define mechanistic aspects of the colitogenic activity of IL-22 observed in our mouse model. Transcripts encoding the neutrophil recruiting chemokines Cxcl1 and Cxcl5 were consistently up-regulated in the colonic tissue of *Cx3cr1^{cre}:Il10ra$^{fl/fl}$ mice* (Fig 2G, F) in an IL-22 dependent manner (Fig 4C). Cxcl1 and Cxcl5 were induced in colonic epithelium, but not expressed by ileal epithelial cells (Fig 2F). In contrast, although induced in the inflamed colon, AMP were constitutively expressed in ileal epithelium. This suggested that neutrophil attraction, rather than AMP induction, might be critical for the

IL-22-driven pathology. In line with this notion, flow cytometry analysis revealed prominent neutrophil infiltrates in the colon of $Cx3cr1^{cre}$:$Il10ra^{fl/fl}$ mice, which were absent in the protected $Cx3cr1^{cre}$: $Il10ra^{fl/fl}$:$Il23a^{fl/fl}$ and $Cx3cr1^{cre}$:$Il10ra^{fl/fl}$:$Il22^{-/-}$ strains (Supp Fig 4, Fig 6A, B). Neutrophils are known to cause collateral tissue damage (46), and their tissue infiltration and activities are tightly controlled (47). In line with their destructive potential, recruited neutrophils in the tissues of $Cx3cr1^{cre}$:$Il10ra^{fl/fl}$ mice displayed elevated ROS production as compared to blood neutrophils of the same animals (Fig 6C).

To formally establish the link between IL-22-expressing CD4^{+} T cells and the neutrophil accumulation, we next tested the impact of a T cell ablation on neutrophil recruitment (Fig 6D). Using an antibody regimen, CD4^{+} T cells were efficiently depleted from mesenteric lymph nodes (LN), while CD8^{+} T cells remained unaffected (Fig 6E). [$Cx3cr1^{cre}$:$Il10ra^{fl/fl}$ > WT] BM chimeras depleted of CD4^{+} T cells showed significant reduction of neutrophil recruitment (Fig 6F). Histological analysis confirmed neutrophil infiltrates in [$Cx3cr1^{cre}$:$Il10ra^{fl/fl}$ > WT] mice and the associated loss of colon tissue architecture, as determined by E-cadherin and collagen staining, which were prevented by the CD4^{+} T cell depletion (Fig 6G). Moreover, reduced neutrophil infiltration was correlated with lower $Il22$, $Cxcl1$ and $Cxcl5$ mRNA expression in BM chimeras depleted of CD4^{+} T cells (Fig 6H). As we found CD4^{+} ILC3, another prominent IL-22 source f.i. during $C. rodentium$ infection (48), to be radiosensitive, these data support the notion that the cellular source of pro-colitic IL-22 in our model are likely Th17 cells (Fig 1E). The depletion experiment places CD4^{+} T cells and IL22 up-stream of neutrophil recruitment in the cascade of colitis progression. Collectively, our observations hence point to IL-22 as a pro-inflammatory factor likely secreted by Th17 cells, inducing EC expression of Cxcl1 and Cxcl5 and promoting neutrophil recruitment to the intestinal $lamina$ $propria$.

Ablation of neutrophil infiltrates ameliorates colitis

As neutrophil recruitment appeared to be a hallmark of macrophage-induced colitis, we next tested the contribution of these cells to tissue pathology. Neutrophil extracellular traps (NETs) were shown to promote inflammation in atherosclerosis and mediate tissue damage created by neutrophils in pulmonary infection (49, 50). However, histological analysis of colitic BM chimeras revealed absence of NET formation in colonic tissue (Supp Fig 6A). To probe for involvement of another prominent neutrophil activity, [$Cx3cr1^{cre}$:$Il10ra^{fl/fl}$ > WT] BM chimeras and controls were treated with neutrophil elastase inhibitor (NEi) (Supp Fig 6B-C). Although we observed a reduction in levels of the neutrophil activation marker CD63 following NEi administration (Supp Fig 6C), the treatment had no effect on neutrophil accumulation and tissue Nos2 levels (Supp Fig 6D, E). Finally, we ablated neutrophils using anti-Ly6G antibody (Fig 7A). Flow cytometry analysis confirmed the depletion of neutrophils from the colon of the antibody-treated [$Cx3cr1^{cre}$:$Il10ra^{fl/fl}$ > WT] BM chimeras (Fig 7B), as did histological analysis (Fig 7C). More importantly, the latter revealed significantly reduced tissue damage in the colons of neutrophil depleted animals, as indicated by absence of villi hypertrophy and loss of cell polarity that was observed in colon areas with high neutrophil infiltrates of the IgG-treated control mice (Fig 7C). Whole tissue RNA analysis by qPCR revealed decreased levels of $Nos2$ expression in neutrophil-depleted BM chimeras (Fig 7D). Of note, also macrophages and EC produced $Nos2$ under

inflammatory conditions according to our RNAseq data (Fig 1A,B; Fig 2F); the fact that neutrophil depletion was sufficient to reduce tissue *Nos2* levels, suggests that these cells are either the main source of this enzyme, or macrophage *Nos2* expression is downstream of neutrophil recruitment. To test for such a potential effect of the neutrophil ablation on macrophage transcriptomes, we performed RNAseq analysis on these cells isolated from anti-Ly6G and control IgGtreated [*Cx3cr1^{cre}:Il10ra$^{fl/fl}$* > WT] BM chimeras (Fig 1A,B; Fig 2F). Neutrophil ablation did not significantly impair macrophage expression of pro-inflammatory factors, such as Nos2, Ccl5 and Saa3 (Fig 7E; Supp Fig 7A); however either the absence of neutrophils or the ensuing improved tissue context did affect the global macrophage transcriptomes (Supp Fig 7B). Collectively, these data establish that the neutrophil recruitment induced by epithelial response to Il22 has a major contribution to tissue damage in IL10R-deficient macrophages driven colitis (Supp Fig 8).

Discussion

Here we focused on understanding the critical steps in the induction and progression of macrophage-driven colitis, as manifested in children and mice harboring IL-10R deficiencies (17, 18). Specifically, macrophages of pediatric patients harboring *IL10Ra* mutations and *Cx3cr1^{cre}:Il10ra$^{fl/fl}$* mice that fail to sense IL-10, develop proinflammatory gene expression signatures that lead to gut pathology.

Using a conditional double mutagenesis strategy we establish macrophagederived IL-23 as critical driver of the disease. Macrophages of *Cx3cr1^{cre}:Il10ra$^{fl/fl}$: Il23a$^{fl/fl}$* mice that lack the ability to produce IL-23 in addition to the IL-10 receptor deficiency, no longer develop a pro-inflammatory gene signature. Our results corroborate and strengthen the key role of IL-23 in colonic inflammation that has been suggested earlier for other experimental models (21, 27, 37). Moreover, we establish a critical hierarchy of pro-inflammatory factors, with macrophage-derived IL-23 at the apex of the cascade. Of note, IL-23 expression in macrophages is tightly controlled, including dedicated post-transcriptional circuits (51, 52) that have been linked to IL-10 (53). Collectively, this highlights IL-23 as a prime target for colitis therapy, as also supported by the clinical success of *Ustekinumab*, a monoclonal antibody that specifically blocks the IL-23 subunit p40 (54, 55).

We found macrophage-derived IL-23 to induce colonic Th17 cells and ILC3 to secrete IL-22, as also suggested in other colitis models (27). However, unlike earlier studies that involved DSS or T cell transfers into lymphopenic mice (29), IL-22 deficient *Cx3cr1^{cre}:Il10ra$^{fl/fl}$* animals were protected from disease, establishing that, akin its role in psoriasis (38), IL-22 production is deleterious in our IBD model. Rather, colitis driven by IL-10R deficient macrophages in animals that harbor normal T cell compartments, and hence probably also IL-10R-deficient pediatric patients, more closely resembles the pathology induced by anti-CD40 treatment (31). The latter model lacks conventional T cells and therefore implies ILC3 as IL-22 source, corroborating an earlier study (56). In contrast, in our model that retains both conventional and unconventional T cells, we assigned IL-22 production to Th17 cells. Interestingly, Shouval and colleagues reported enhanced Th17 Responses in patients with IL10R deficiency and infantile-onset IBD (57), the close human counterpart of our model (17, 18). The pathogenicity of Th17 cells was also highlighted in a

recent study that reported a direct link between *H. hepaticus* colonization and the generation of these cells (58). *H. hepaticus* infection of IL-10 deficient mice induced inflammatory Th17 cells in the colon but not the ileum, in line with the notion that IBD pathology is restricted to the large intestine in both IL-10-deficient and *Cx3cr1^{cre}:Il10ra$^{fl/fl}$* mice. Collectively, our study and the one by Littman and colleagues (58) highlight the importance to investigate key drivers of IBD pathology also in models that retain conventional T cells, in addition to lymphopenic or immuno-deficient mice.

A pro-inflammatory role of IL-22 has been identified in skin pathologies, such as acanthosis and psoriasis (38) and was suggested to be related to keratinocyte hyperplasia. In the context of the gut, *Salmonella enterica ser. Typhimurium* was shown to benefit from IL-22 induction, since EC-derived AMP provided a competitive colonization advantage for the pathogen (59). As to the mechanism how IL-22 promotes inflammation, the data point to a critical role of EC-derived neutrophil chemo-attractants in our model. Specifically, Th17 derived IL-22 induces EC to express the chemokines Cxcl1 and Cxcl5 alongside AMP (60). The observed tight link between neutrophil infiltrates and gut pathology in the Cx3cr1^{cre}:Il10ra$^{fl/fl}$ mouse colitis model suggests that these factors are a major component in its pathological cascade, as recently proposed for the anti-CD40 colitis model (31).

Taken together, this study provides mechanistic insight into the cascade of inter-cellular communication events triggered by Il10R deficient macrophages in the colon. IL-23 produced by the mutant cells emerged as critical trigger of Th17 cells that secrete IL-22 and thereby initiate an epithelial cell response that results in deleterious recruitment of neutrophils. Our findings might have direct implications for pediatric patients harboring *IL10R* mutations (17, 18) and add to our general understanding of cell type-specific contributions to IBD pathology.

Materials and Methods

Mice

This study included the following animals: *Cx3cr1^{cre}* mice (JAX stock # 025524 B6J.B6N(Cg)-*Cx3cr1$^{tm1.1(cre)Jung}$*/J (61), *Il-10ra$^{fl/fl}$* mice (62), *Il-23a$^{fl/fl}$* mice (44), *Rorgt^{gfp}* reporter mice (40), *R26-tdTomato* mice (B6.Cg-*Gt(ROSA)26Sor$^{tm9(CAG-tdTomato)Hze}$*/J) (63), Villin^{cre} mice (42) and *Il22$^{-/-}$* mice (39). Only male mice were used. BM chimeras were generated by engraftment of recipient mice that were irradiated the day before with a single dose of 950 cGy using a XRAD 320 machine (Precision XRay (PXI). All animals were on C57Bl/6 background and bred at the Weizmann animal facility. Sentinels in our facility were typed *Helicobacter hepaticus* positive. Whenever possible, age matched co-housed males were used for experiments. Animals were maintained under specific pathogen-free conditions and handled according to protocols approved by the Weizmann Institute Animal Care Committee as per international guidelines.

Cell isolation, flow cytometry analysis and sorting of intestinal macrophages and intestinal epithelial cells

For the isolation of colonic EC, extra-intestinal fat tissue and blood vessels were carefully removed and colons were then flushed of their luminal content with cold PBS, opened longitudinally, and cut into 0.5 cm pieces. Colon pieces were incubated in RPMI medium supplemented with 2mM EDTA, 10%FBS, 1% PenStrep and 1% Sodium pyruvate for 40 minutes at 37°C shaking at 250 rpm.

For the isolation of colonic *lamina propria* cells, EC and mucus were removed by 40 min incubation with HBSS (without Ca2+ and Mg2+) containing 5% FBS, 2 mM EDTA, and 0.15 mg/ml (1 mM) DTT (Sigma) at 37°C shaking at 250 rpm. Colon pieces were then digested in PBS+/+ containing 5% FBS, 1 mg/ml Collagenase VIII (Sigma), and 0.1 mg/ml DNase I (Roche) for 40 min at 37°C shaking at 250 rpm. The digested cell suspension was then washed with PBS and passed sequentially through 100 and 40 mm cell strainers. Antibodies were used to stain the surface markers of the cells: CD45 (30-F11), Ly-6C (HK1.4), CD11b (M1/70), CD11c (HL3), Ly6G (1A8), CD64 (X54-5/7.1) from Biolegend, Bio-gems or eBioscience, CD103 (M290) from BD biosciences. Cells were analyzed with LSRFortessa flow cytometer (BD) or sorted using a FACSAria machine (BD). Flow cytometry analysis was done with the FlowJo software.

Real time PCR

Total RNA was extracted from sorted cells with RNeasy Micro Kit (Qiagen) and from murine colons with PerfectPure RNA Tissue Kit (5 PRIME). RNA was reverse transcribed with a mixture of random primers and oligo-dT with a High-Capacity cDNA Reverse Transcription Kit (Applied Biosystems). PCR was performed with SYBR Green PCR Master Mix kit (Applied Biosystems). Quantification of the PCR signals of each sample was performed by comparing the cycle threshold values (Ct), in duplicate, of the gene of interest with the Ct values of the TATA-binding protein (TBP) housekeeping gene (for whole tissue RNA) or actin-b (for sorted cells). Primers used for qPCR:

Gene	Fw (5'->3')	Rev (5'->3')
Actb	GGAGGGGGGTTGAGGTGTT	TGTGCACTTTTATTGGTCTCA
TBP	GAAGCTGCGGTACAATTCCAG	CCCCTTGTACCCTTCACCAAT
Reg3b	ACTCCCTGAAGAATATACCCTCC	CGCTATTGAGCACAGATACGAG
Reg3g	ATGCTTCCCCGTATAACCATCA	GGCCATATCTGCATCATACCAG
Nos2	CTGCAGCACTTGGATCAGGAACCTG	GGGAGTAGCCTGTGTGCACCTGGAA
Il22	ATGAGTTTTTCCCTTATGGGGAC	GCTGGAAGTTGGACACCTCAA
Il23	ATGCTGGATTGCAGAGCAGTA	ACGGGGGCACATTATTTTTAGTCT
Ccl5	AGATCTCTGCAGCTGCCCTCA	GGAGCACTTGCTGCTGGTGTAG
Cxcl5	TGCGTTGTGTTTGCTTAACCG	CTTCCACCGTAGGGCACTG
Cxcl1	GACCATGGCTGGGATTCACC	GTGTGGCTATGACTTCGGTT

RNA sequencing and analysis

EC mRNA sequencing was conducted with the help of the INCPM unit at the Weizmann institute of Science – total RNA was extracted from $0.1\text{-}1*10^6$ sorted cells with RNeasy Micro Kit (Qiagen). 100 ng of total RNA was processed using the TruSeq Stranded Total RNA HTSample Prep Kit (with Ribo-Zero Gold) of Illumina (RS-122-2303). Libraries were evaluated by Qubit and TapeStation. Sequencing libraries were constructed with barcodes to allow multiplexing of 24 samples ran on 3 lanes. ~20 million single-end 50-bp reads were sequenced per sample on Illumina HiSeq 2500 high output mode instrument.

Macrophage mRNA was sequenced using MARSeq, as previously described (64). Briefly, 10^4–10^5 cells from each population were sorted into 50 μl of lysis/binding buffer (Life Technologies). mRNA was captured with 15 μl of Dynabeads oligo(dT) (Life Technologies), washed, and eluted at 85°C with 6 μl of 10 mM Tris-Cl (pH 7.5). ~5 million reads were sequenced per library. In both cases gene expression levels were calculated using the HOMER software package (analyzeRepeats.pl rna mm9 -d <tagDir> -count exons -condenseGenes -strand + -raw) (65). Normalization and differential expression analysis was done using the DESeq2 R-package,

Histopathological analysis

Analysis was performed as previously described with minor adjustments (19). Briefly, Colon was fixed in 2% PFA solution overnight at 4°C, then embedded in paraffin, sectioned and stained with H&E. Tissues were examined in a blinded manner by a pathologist. Three segments of the colon (proximal colon, medial colon and distal colon-rectum) were given a score between 0-4 and the average of these scores provided a total colonic disease score.

Immunohistochemistry

For T cell and ILC3 staining, tissues were fixed in 2% paraformaldehyde at 4°C and stained for CD3 (SP7,abcam) and GFP (polyclonal IgG ab6658,abcam) overnight in 4°C. Alexa-fluor 488-conjugated donkey anti-goat and Cy3-conjugated donkey anti-rabbit (Jackson ImmunoResearch) secondary antibodies were added for 1 hour. Nuclei were stained with Hoechst. Images were acquired using a Nikon Eclipse Ti inverted spinning-disc confocal microscope with 20× air objectives, with Andor iQ software and analyzed with Volocity 6.1.1 software (Improvision Ltd).

For neutrophil and tissue damage staining after de-waxing and re-hydrating, the formalin fixed, paraffin embedded Gut sections were incubated in Target Retrieval solution pH 9.0 (S236884-2, Agilent Technologies LDA UK Limited) at 97C for 45 min. Sections were incubated with primary antibodies mouse anti E-Cadherin Ab (610181, BD Biosciences, 1:500 dilution) and Rabbit polyclonal to Collagen IV (ab6586, ABCAM PLC, 1:500 dilution) followed by Alexa Fluor 488–conjugated donkey anti-mouse (A21202, Thermo Fisher Scientific (Life Technologies), 1:200 dilution), Alexa Fluor 568–conjugated donkey anti rabbit, Alexa Fluor 647 - conjugated anti - Ly6G and DAPI. Then tissues were mounted with ProLong Gold Antifade Mountant (P36934, Thermo Fisher Scientific (Life Technologies) and examined with confocal microscopy. Image analysis was performed using ImageJ.

Antibiotics treatment

For antibiotic treatment, mice were given a combination of vancomycin (0.5 g/l), ampicillin (1 g/l), kanamycin (1 g/l), and metronidazole (1 g/l) in their drinking water upon weaning and continuously until they were sacrificed. All antibiotics were obtained from Sigma Aldrich.

In vivo cell depletion and NEi treatment

For CD4 depletion mice were injected i.v. with 100μg of anti-CD4 antibody (Bioxcell, clone GK1.5) or isotype control (Bioxcell, clone LTF2). For neutrophil depletion mice were injected i.p. with 120μg of anti-Ly6g antibody (Bioxcell clone 1A8) or rat serum IgG control (Sigma Aldrich). Neutrophil elastase inhibitor (NEi) was purchased from axon medchem and injected i.p. at 2.5 μg/g every three days.

Quantification and statistical analysis

In all experiments, data are presented as mean if not stated otherwise, each dot represents one mouse. Statistical tests were selected based on appropriate assumptions with respect to data distribution and variance characteristics. Student's t test (two-tailed) was used for the statistical analysis of differences between two groups. One-way Anova followed by Bonferroni correction was used for the statistical analysis of differences between three or more groups. Statistical significance was defined as $P<0.05$. Sample sizes were chosen according to standard guidelines. Number of animals is indicated as 'n'. Of note, sizes of the tested animal groups were also dictated by availability of the transgenic strains and litter sizes, allowing littermate controls. Pre-established exclusion criteria are based on IACUC guidelines. Animals of the same age, sex and genetic background were randomly assigned to treatment groups. The investigator was not blind to the mouse group allocation. Tested samples were blindly assayed.

Supplementary Material

Refer to Web version on PubMed Central for supplementary material.

Acknowledgments

References

1. Manolio TA, et al. Finding the missing heritability of complex diseases. Nature. 2009; 461:747–753. [PubMed: 19812666]

2. Huang H, et al. Fine-mapping inflammatory bowel disease loci to single-variant resolution. Nature. 2017; 547:173–178. [PubMed: 28658209]

3. Joeris T, Müller-Luda K, Agace WW, Mowat AM. Diversity and functions of intestinal mononuclear phagocytes. Mucosal Immunol. 2017; 10:845–864. [PubMed: 28378807]

4. Sonnenberg GF, Artis D. Innate lymphoid cells in the initiation, regulation and resolution of inflammation. Nat Med. 2015; 21:698–708. [PubMed: 26121198]

5. Mortha A, et al. Microbiota-dependent crosstalk between macrophages and ILC3 promotes intestinal homeostasis. Science. 2014; 343:1249288–1249288. [PubMed: 24625929]

6. Levy, M, Kolodziejczyk, AA, Thaiss, CA, Elinav, E. Vol. 17. Nature Publishing Group; 2017. Dysbiosis and the immune system; 219–232.

7. Maloy KJ, Powrie F. Intestinal homeostasis and its breakdown in inflammatory bowel disease. Nature. 2011; 474:298–306. [PubMed: 21677746]

8. Takeda K, et al. Enhanced Th1 activity and development of chronic enterocolitis in mice devoid of Stat3 in macrophages and neutrophils. Immunity. 1999; 10:39–49. [PubMed: 10023769]

9. Shouval DS, et al. Interleukin 10 receptor signaling: master regulator of intestinal mucosal homeostasis in mice and humans. Adv Immunol. 2014; 122:177–210. [PubMed: 24507158]

10. Varol C, Mildner A, Jung S. Macrophages: development and tissue specialization. Annu Rev Immunol. 2015; 33:643–675. [PubMed: 25861979]

11. Varol C, et al. Intestinal lamina propria dendritic cell subsets have different origin and functions. Immunity. 2009; 31:502–512. [PubMed: 19733097]

12. Bogunovic M, et al. Origin of the Lamina Propria Dendritic Cell Network. Immunity. 2009; 31:513–525. [PubMed: 19733489]

13. Bain CC, et al. Constant replenishment from circulating monocytes maintains the macrophage pool in the intestine of adult mice. Nat Immunol. 2014; doi: 10.1038/ni.2967

14. Shaw TN, et al. Tissue-resident macrophages in the intestine are long lived and defined by Tim-4 and CD4 expression. J Exp Med. 2018; 7

15. Zigmond E, Jung S. Intestinal macrophages: well educated exceptions from the rule. Trends in Immunology. 2013; 34:162–168. [PubMed: 23477922]

16. Rubtsov YP, et al. Regulatory T cell-derived interleukin-10 limits inflammation at environmental interfaces. Immunity. 2008; 28:546–558. [PubMed: 18387831]

17. Glocker E-O, et al. Inflammatory Bowel Disease and Mutations Affecting the Interleukin-10 Receptor. N Engl J Med. 2009; 361:2033–2045. [PubMed: 19890111]

18. Shouval DS, et al. Interleukin-10 receptor signaling in innate immune cells regulates mucosal immune tolerance and anti-inflammatory macrophage function. Immunity. 2014; 40:706–719. [PubMed: 24792912]

19. Zigmond E, et al. Macrophage-Restricted Interleukin-10 Receptor Deficiency, but Not IL-10 Deficiency, Causes Severe Spontaneous Colitis. Immunity. 2014; 40:720–733. [PubMed: 24792913]

20. Langrish CL, et al. IL-12 and IL-23: master regulators of innate and adaptive immunity. Immunol Rev. 2004; 202:96–105. [PubMed: 15546388]

21. Hue S, et al. Interleukin-23 drives innate and T cell-mediated intestinal inflammation. J Exp Med. 2006; 203:2473–2483. [PubMed: 17030949]

22. Kullberg MC, et al. IL-23 plays a key role in Helicobacter hepaticus-induced T cell-dependent colitis. J Exp Med. 2006; 203:2485–2494. [PubMed: 17030948]

23. Ahern PP, et al. Interleukin-23 drives intestinal inflammation through direct activity on T cells. Immunity. 2010; 33:279–288. [PubMed: 20732640]

24. Kinnebrew MA, et al. Bacterial flagellin stimulates Toll-like receptor 5-dependent defense against vancomycin-resistant Enterococcus infection. J Infect Dis. 2010; 201:534–543. [PubMed: 20064069]

25. Aychek T, et al. IL-23-mediated mononuclear phagocyte crosstalk protects mice from Citrobacter rodentium-induced colon immunopathology. Nat Comms. 2015; 6

26. Longman RS, et al. CX3CR1+ mononuclear phagocytes support colitis-associated innate lymphoid cell production of IL-22. J Exp Med. 2014; 9:143.

27. Arnold IC, et al. CD11c(+) monocyte/macrophages promote chronic Helicobacter hepaticus-induced intestinal inflammation through the production of IL-23. Mucosal Immunol. 2016; 9:352–363. [PubMed: 26242598]

28. Sugimoto K, et al. IL-22 ameliorates intestinal inflammation in a mouse model of ulcerative colitis. J Clin Invest. 2008; 118:534–544. [PubMed: 18172556]

29. Zenewicz LA, et al. Innate and adaptive interleukin-22 protects mice from inflammatory bowel disease. Immunity. 2008; 29:947–957. [PubMed: 19100701]

30. Sabat R, Ouyang W, Wolk K. Therapeutic opportunities of the IL-22–IL-22R1 system. Nat Rev Drug Discov. 2014; 13:21–38. [PubMed: 24378801]

31. Eken A, Singh AK, Treuting PM, Oukka M. IL-23R+ innate lymphoid cells induce colitis via interleukin-22-dependent mechanism. Mucosal Immunol. 2013; 7:143–154. [PubMed: 23715173]

32. Sonnenberg GF, et al. Pathological versus protective functions of IL-22 in airway inflammation are regulated by IL-17A. Journal of Experimental Medicine. 2010; 207:1293–1305. [PubMed: 20498020]

33. Wolk K, et al. Deficient cutaneous antibacterial competence in cutaneous T-cell lymphomas: role of Th2-mediated biased Th17 function. Clin Cancer Res. 2014; 20:5507–5516. [PubMed: 25212608]

34. Mizoguchi A. Healing of intestinal inflammation by IL-22. Inflamm Bowel Dis. 2012; 18:1777–1784. [PubMed: 22359410]

35. Zigmond E, et al. Infiltrating monocyte-derived macrophages and resident kupffer cells display different ontogeny and functions in acute liver injury. The Journal of Immunology. 2014; 193:344–353. [PubMed: 24890723]

36. Duerr RH, et al. A genome-wide association study identifies IL23R as an inflammatory bowel disease gene. Science. 2006; 314:1461–1463. [PubMed: 17068223]

37. Yen D, et al. IL-23 is essential for T cell–mediated colitis and promotes inflammation via IL-17 and IL-6. J Clin Invest. 2006; 116:1310–1316. [PubMed: 16670770]

38. Zheng Y, et al. Interleukin-22, a TH17 cytokine, mediates IL-23-induced dermal inflammation and acanthosis. Nature. 2006; 445:648–651. [PubMed: 17187052]

39. Zheng Y, et al. Interleukin-22 mediates early host defense against attaching and effacing bacterial pathogens. Nat Med. 2008; 14:282–289. [PubMed: 18264109]

40. Eberl G, et al. An essential function for the nuclear receptor RORγt in the generation of fetal lymphoid tissue inducer cells. Nat Immunol. 2003; 5:64–73. [PubMed: 14691482]

41. Satoh-Takayama N, et al. The Chemokine Receptor CXCR6 Controls the Functional Topography of Interleukin-22 Producing Intestinal Innate Lymphoid Cells. Immunity. 2014; 41:776–788. [PubMed: 25456160]

42. el Marjou F, et al. Tissue-specific and inducible Cre-mediated recombination in the gut epithelium. genesis. 2004; 39:186–193. [PubMed: 15282745]

43. Hua G, et al. Crypt base columnar stem cells in small intestines of mice are radioresistant. Gastroenterology. 2012; 143:1266–1276. [PubMed: 22841781]

44. Thakker P, et al. IL-23 is critical in the induction but not in the effector phase of experimental autoimmune encephalomyelitis. J Immunol. 2007; 178:2589–2598. [PubMed: 17277169]

45. Zindl CL, et al. IL-22-producing neutrophils contribute to antimicrobial defense and restitution of colonic epithelial integrity during colitis. Proceedings of the National Academy of Sciences. 2013; 110:12768–12773.

46. Fournier BM, Parkos CA. The role of neutrophils during intestinal inflammation. Mucosal Immunol. 2012; 5:354–366. [PubMed: 22491176]

47. Grainger JR, et al. Inflammatory monocytes regulate pathologic responses to commensals during acute gastrointestinal infection. Nat Med. 2013; 19:713–721. [PubMed: 23708291]

48. Ahlfors H, et al. IL-22 Fate Reporter Reveals Origin and Control of IL-22 Production in Homeostasis and Infection. J Immunol. 2014; 193:4602–4613. [PubMed: 25261485]

49. Warnatsch A, et al. Neutrophil extracellular traps license macrophages for cytokine production in atherosclerosis. Science. 2015; 349:316–320. [PubMed: 26185250]

50. Branzk N, et al. Neutrophils sense microbe size and selectively release neutrophil extracellular traps in response to large pathogens. Nat Immunol. 2014; 15:1017–10251. [PubMed: 25217981]

51. Molle C, et al. Tristetraprolin regulation of interleukin 23 mRNA stability prevents a spontaneous inflammatory disease. J Exp Med. 2013; 210:1675–1684. [PubMed: 23940256]

52. Brooks SA, Blackshear PJ. Tristetraprolin (TTP): interactions with mRNA and proteins, and current thoughts on mechanisms of action. Biochim Biophys Acta. 2013; 1829:666–679. [PubMed: 23428348]

53. Gaba A, et al. Cutting edge: IL-10-mediated tristetraprolin induction is part of a feedback loop that controls macrophage STAT3 activation and cytokine production. The Journal of Immunology. 2012; 189:2089–2093. [PubMed: 22865915]

54. Feagan BG, et al. Ustekinumab as Induction and Maintenance Therapy for Crohn's Disease. N Engl J Med. 2016; 375:1946–1960. [PubMed: 27959607]

55. Sandborn WJ, et al. Ustekinumab Induction and Maintenance Therapy in Refractory Crohn's Disease. N Engl J Med. 2012; 367:1519–1528. [PubMed: 23075178]

56. Buonocore S, et al. Innate lymphoid cells drive interleukin-23-dependent innate intestinal pathology. Nature. 2010; 464:1371–1375. [PubMed: 20393462]

57. Shouval DS, et al. Enhanced TH17 Responses in Patients with IL10 Receptor Deficiency and Infantile-onset IBD. Inflamm Bowel Dis. 2017; 23:1950–1961. [PubMed: 29023267]

58. Xu M, et al. c-MAF-dependent regulatory T cells mediate immunological tolerance to a gut pathobiont. Nature. 2018; 554:373–377. [PubMed: 29414937]

59. Behnsen J, et al. The Cytokine IL-22 Promotes Pathogen Colonization by Suppressing Related Commensal Bacteria. Immunity. 2014; 40:262–273. [PubMed: 24508234]

60. Aujla SJ, et al. IL-22 mediates mucosal host defense against Gram-negative bacterial pneumonia. Nat Med. 2008; 14:275–281. [PubMed: 18264110]

61. Yona S, et al. Fate mapping reveals origins and dynamics of monocytes and tissue macrophages under homeostasis. Immunity. 2013; 38:79–91. [PubMed: 23273845]

62. Pils MC, et al. Monocytes/macrophages and/or neutrophils are the target of IL-10 in the LPS endotoxemia model. Eur J Immunol. 2010; 40:443–448. [PubMed: 19941312]

63. Madisen L, et al. nn.2467. Nat Neurosci. 2009; 13:133–140. [PubMed: 20023653]

64. Jaitin DA, et al. Massively parallel single-cell RNA-seq for marker-free decomposition of tissues into cell types. Science. 2014; 343:776–779. [PubMed: 24531970]

65. Heinz S, et al. Simple Combinations of Lineage-Determining Transcription Factors Prime cis-Regulatory Elements Required for Macrophage and B Cell Identities. Molecular Cell. 2010; 38:576–589. [PubMed: 20513432]
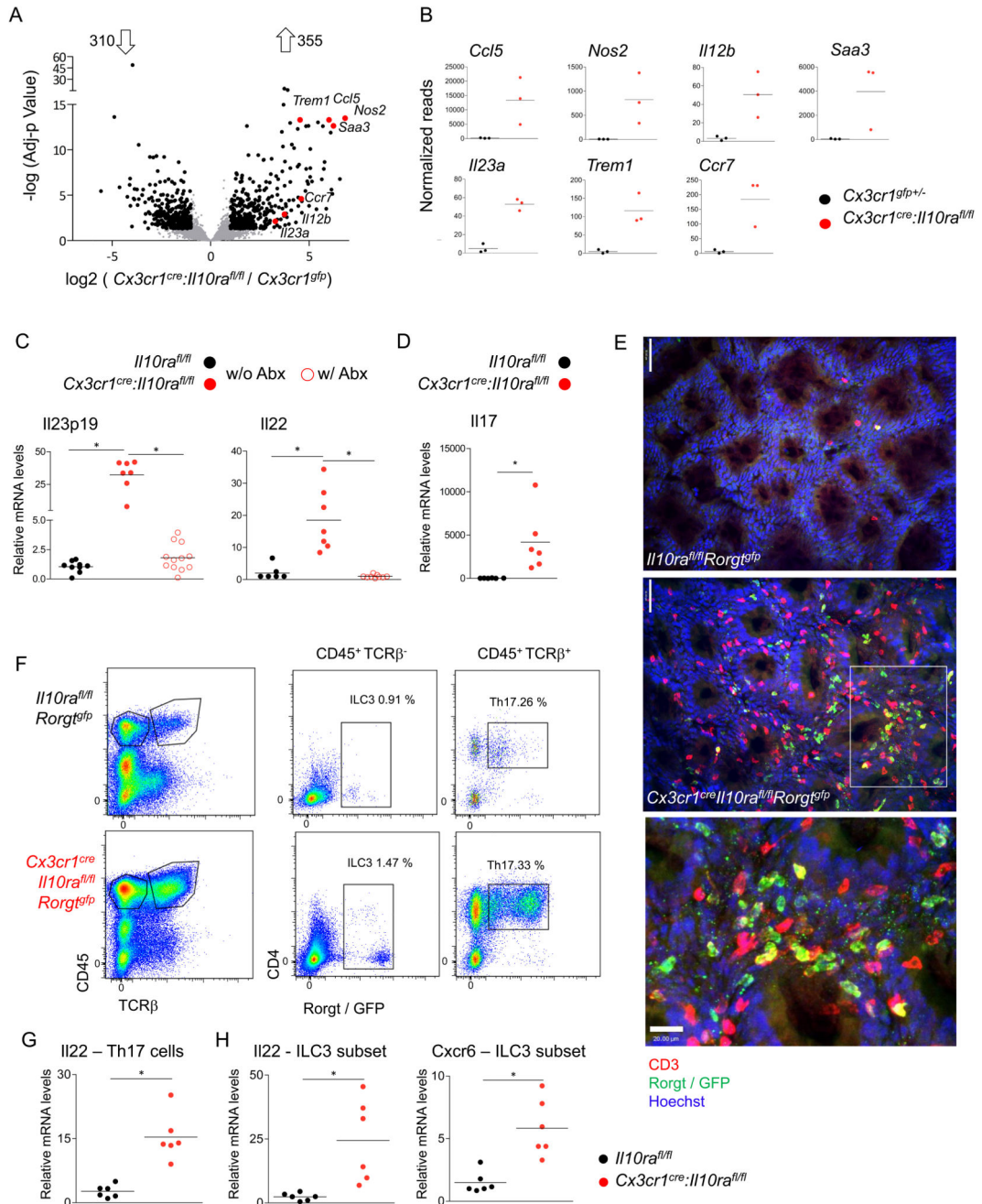
Figure 1. IL-10 receptor-deficient macrophages secrete IL-23, inducing IL-22 secretion by ILC3 and Th17 cells.

(A) Volcano plot of statistical significance (-$\log_{10}$ p-value) against log 2 ratio of macrophages sorted from the colonic *lamina propria* of 6-7 weeks old *Cx3cr1^cre^Il10ra^fl/fl^* and Cx3cr1^gfp/+^ mice, based on RNA-seq data. Significantly up or down regulated genes (fold change>2, adj-p value<0.05) are in black, relevant pro inflammatory up-regulated genes are highlighted in red. Data are representative of two independent experiment, n>=3 for each group.

(B) RNA-seq normalized read numbers for single genes of interest are plotted separately, each dot represents one mouse.

(C) qRT-PCR analysis of il23p19 expression by sorted colonic MFs from 6-7 weeks old mice (left), or of il22 expression (right) in colonic whole tissue extracts of 6-7 weeks old mice. Data collected from two independent experiments, n>=3 in each.

(D) qRT-PCR analysis of il17 expression in colonic whole tissue extracts of indicated mice. Data collected from two independent experiments, n>=3 in each.

(E) Whole mount staining of colonic tissue of *Cx3cr1^{cre}:Il10ra$^{fl/fl}$:Rorgt^{gfp}* mice and Cre negative littermates (age 3-4 months), analysed by confocal microscope, GFP in green, CD3 in red. Indent in the bottom is in the white rectangle, Th17 marked with full arrow, ILC3 dashed arrow. Top scale=50μm, bottom scale= 20μm.

(F) Representative picture of flow cytometry analysis and sorting strategy of *Cx3cr1^{cre}:Il10ra$^{fl/fl}$:Rorgt^{gfp}* mice and Cre negative littermates 3-4 months old.

(G-H) qRT-PCR analysis of RNA extracted from sorted colonic Th17 cells (F) or ILC3 (G) for indicated genes. Data are collected from two independent experiments, n=3 in each.
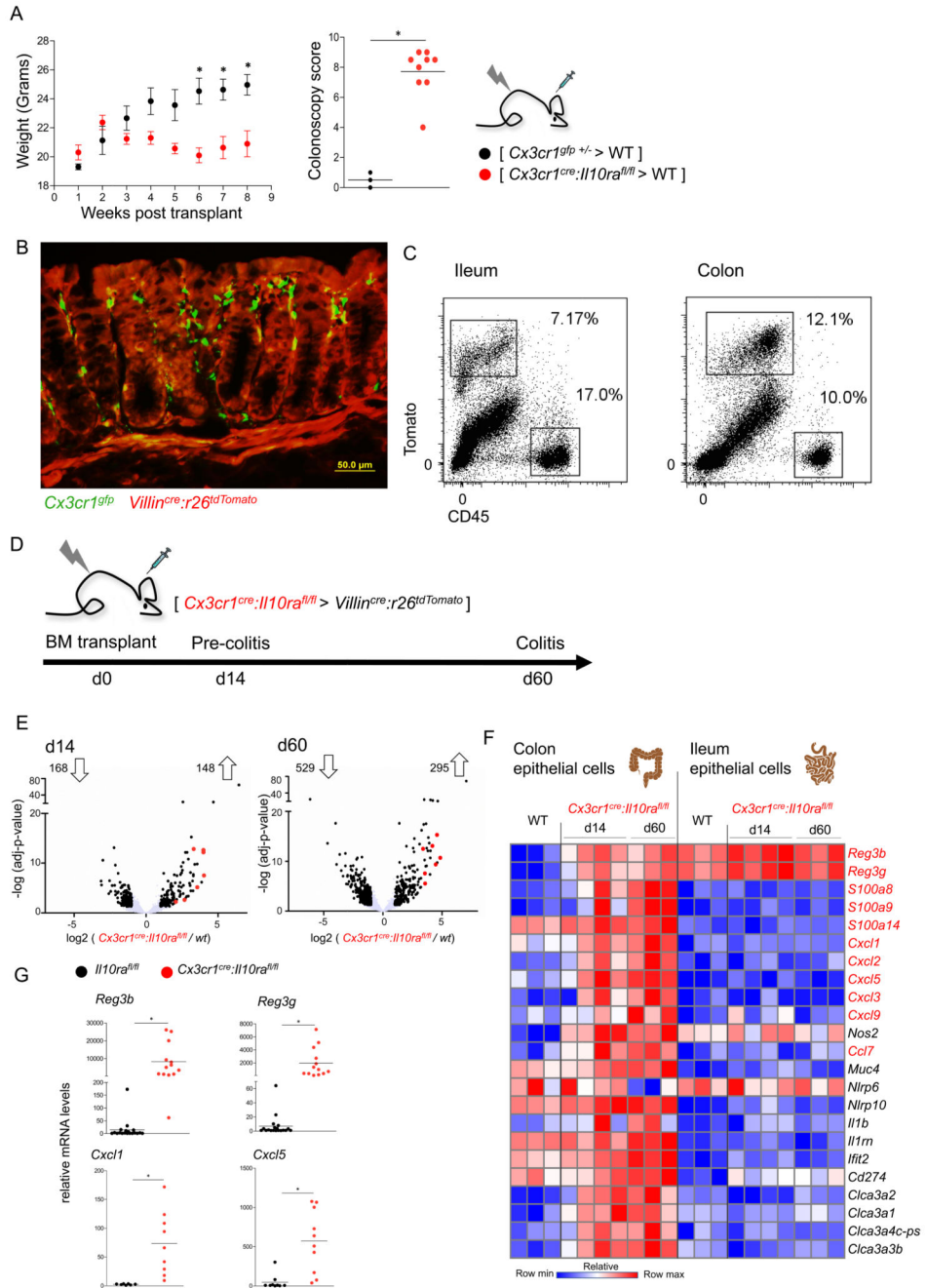
Figure 2. The response of epithelial cells to pro-inflammatory macrophages.

(**A**) Weight and colonoscopic analysis of *[Cx3cr1^{cre}:Il10ra$^{fl/fl}$ >* WT] or *[Cx3cr1$^{gfp/+}$ >* WT] BM chimeras. Colonoscopy was performed 7 weeks post-transplant. Data are representative of 3 independent experiments, n>=3 for each group. *p<0.05.

(**B**) Representative picture of microscopic analysis of [*Cx3cr1^{gfp}>Villin^{cre}:R26-tdTomato*] BM chimera.

(**C**) Representative picture of flow cytometry analysis and sorting strategy of epithelial cells from [*Cx3cr1^{gfp}>Villin^{cre}:R26-tdTomato*] BM chimera.

(D) Description of BM chimera experiment and timeline of epithelial cell harvest.

(E) Volcano plot of statistical significance (log10 p-value) against log 2 ratio of epithelial cells sorted from the colon of *[Cx3cr1^{cre}il10ra$^{fl/lf}$ >Villin^{cre}:R26-tdTomato]* BM chimeras *and Villin^{cre}:R26-tdTomato* mice, based on RNA-seq data. Significantly up or down regulated genes (fold change>2, adj-p value<0.05) are in black, il22 induced genes are highlighted in red. Data are from one experiment, n>=3 for each group.

(F) Heatmap of RNAseq data of colonic and ileal epithelial cells extracted from the same mouse. Normalized reads number were log transformed. Presented are genes of interest, significantly upregulated in colonic but not ileal epithelial cells in response to pro-inflammatory macrophages at both disease stages (d14 and d60 post-transplant).

(G) qRT-PCR analysis of *reg3b*, *reg3g*, *cxcl1* and *cxcl5* expression in whole tissue extracts of colons of 6-7 weeks old mice. Data collected from two independent experiments, n>=3 in each.
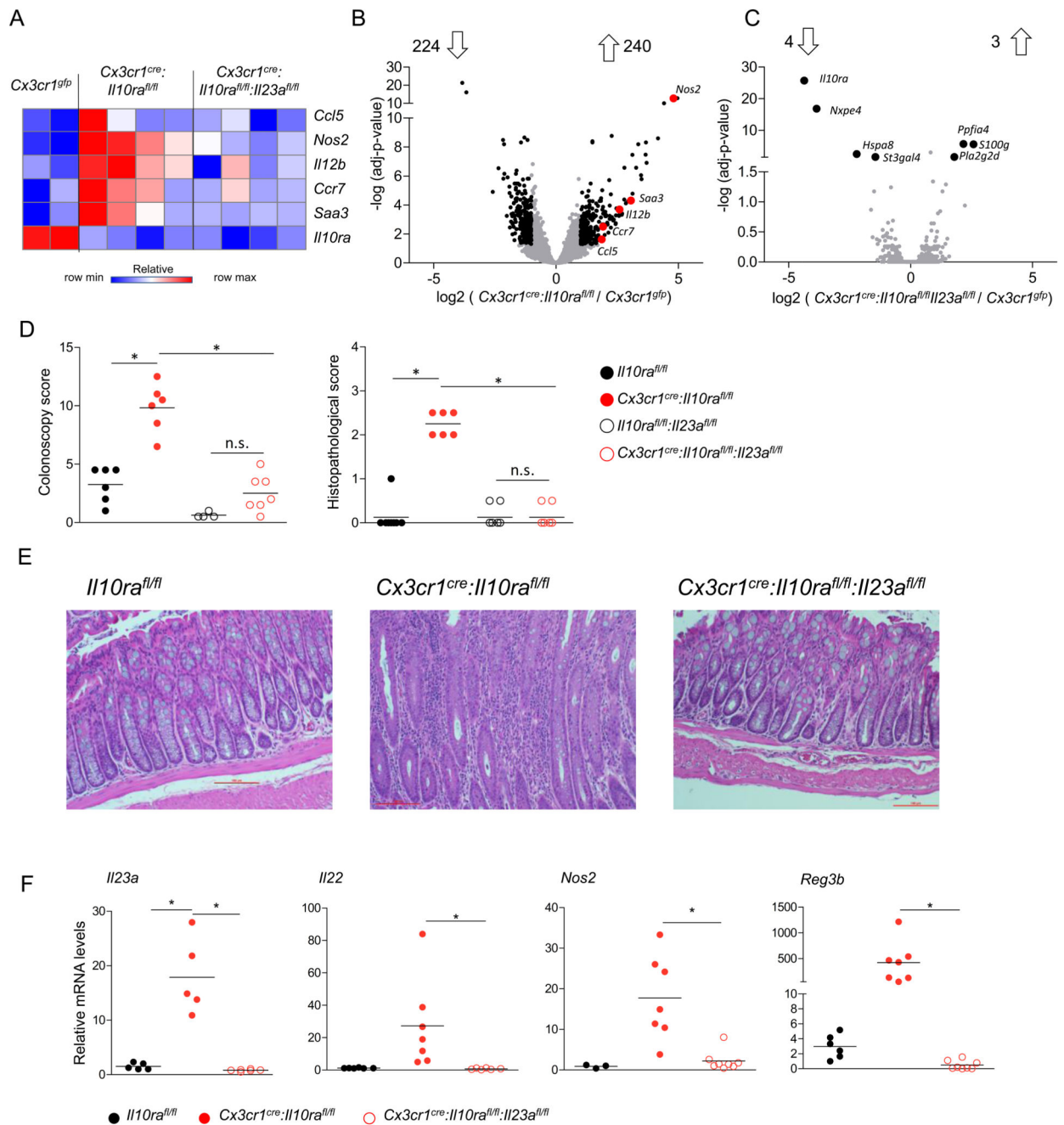
Figure 3. IL-23 deficiency prevents the colitogenic activity of IL-10 receptor-mutant macrophages.

(A) Heatmap of RNAseq data of colonic macrophages sorted from 6-7 weeks old mice. Normalized reads number were log transformed.

(B-C) Volcano plot of statistical significance (log10 p-value) against log 2 ratio of macrophages sorted from the colonic *lamina propria* of B - *Cx3cr1*[cre]:*Il10ra*^{fl/fl} and Cx3cr1[gfp/+] mice or C - *Cx3cr1*[cre]:*Il10ra*^{fl/fl}:*Il23a*^{fl/fl} and *Cx3cr1*[gfp/+] mice, based on RNA-seq data. Significantly up or down regulated genes (fold change>2, adj-p value<0.05) are in

black, relevant pro inflammatory up-regulated genes are highlighted in red. In (B) Data are representative of two independent experiment (B) or from one experiment (C), in each experiment n>=3 for each group.

(D) Colonoscopic (left) and histopathological (right) analysis of 3-4 months old mice. Data are collected from two independent experiments, n>=3 in each.

(E) Representative images of histopathological analysis of indicated mouse strains.

(F) qRT-PCR analysis of *il23a* expression by sorted colonic macrophages of indicated mouse strains (left), or *il22,* nos2 and reg3b expression in colonic whole tissue RNA extracts of indicated mouse strains. Data are collected from two independent experiments, n>=3 in each. All mice were age matched; each dot represents one mouse.

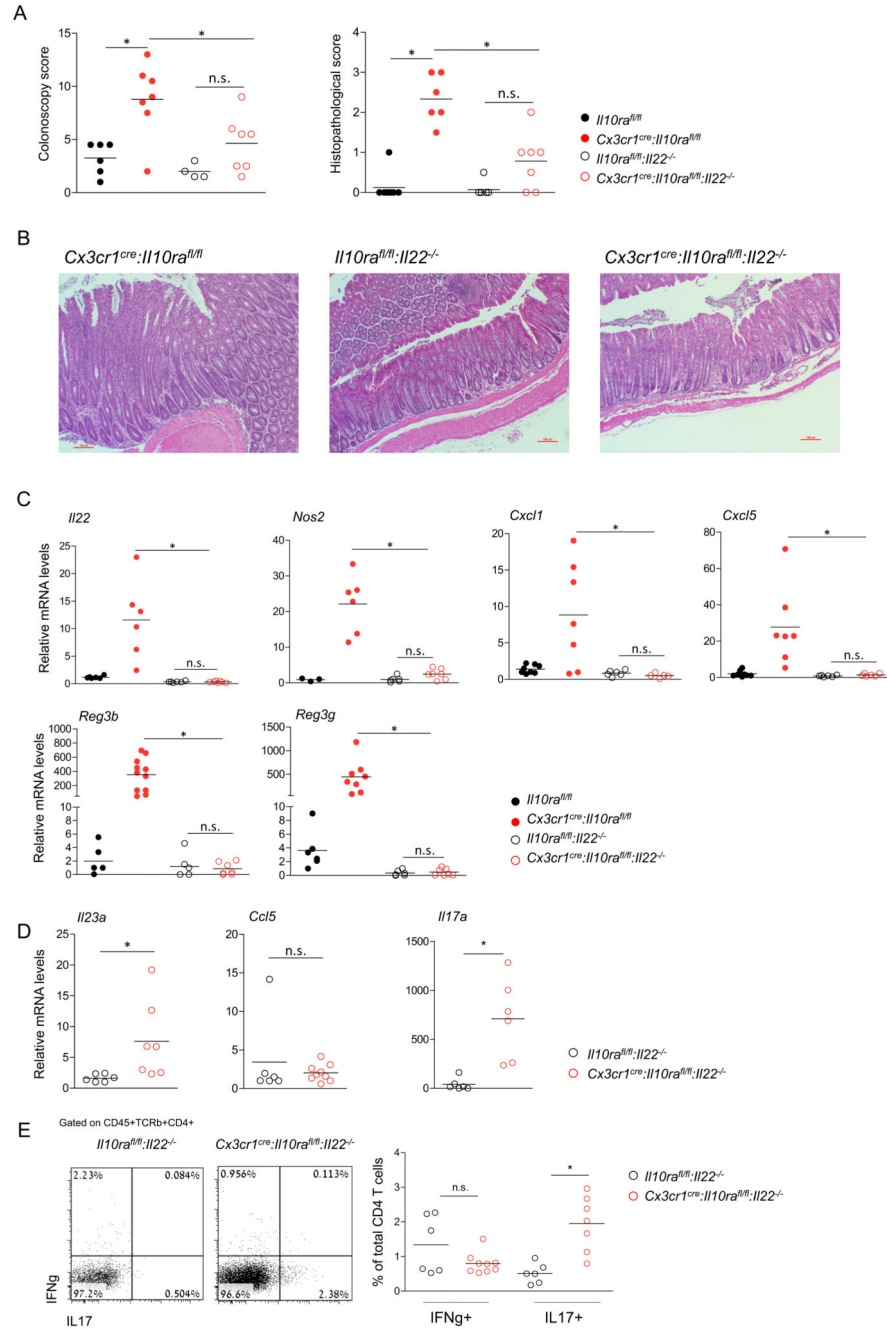**Figure 4. IL-22 is critical for colitis driven by IL-10 receptor-deficient macrophages.**
(A) Colonoscopic (left) and histopathological (right) analysis of 3-4 months old mice.
(B) Representative images of histopathological analysis of indicated mouse strains.
(C) qRT-PCR analysis of *il22*, *cxcl1*, *cxcl5*, *reg3b*, *reg3g* and *nos2* expression in colonic whole tissue extracts of indicated mouse strains.
(D) qRT-PCR analysis of *il23a* and *Ccl5* by sorted colonic macrophages of indicated mouse strains (left), and whole tissue *il17a* levels of indicated mouse strains

(E) Flow cytometry analysis and quantification of lamina propria T cells extracted from the colons of indicated mouse strains.

Data in A,C,D and E are collected from two independent experiments, n>=3 in each. All mice were age matched, each dot represents one mouse.
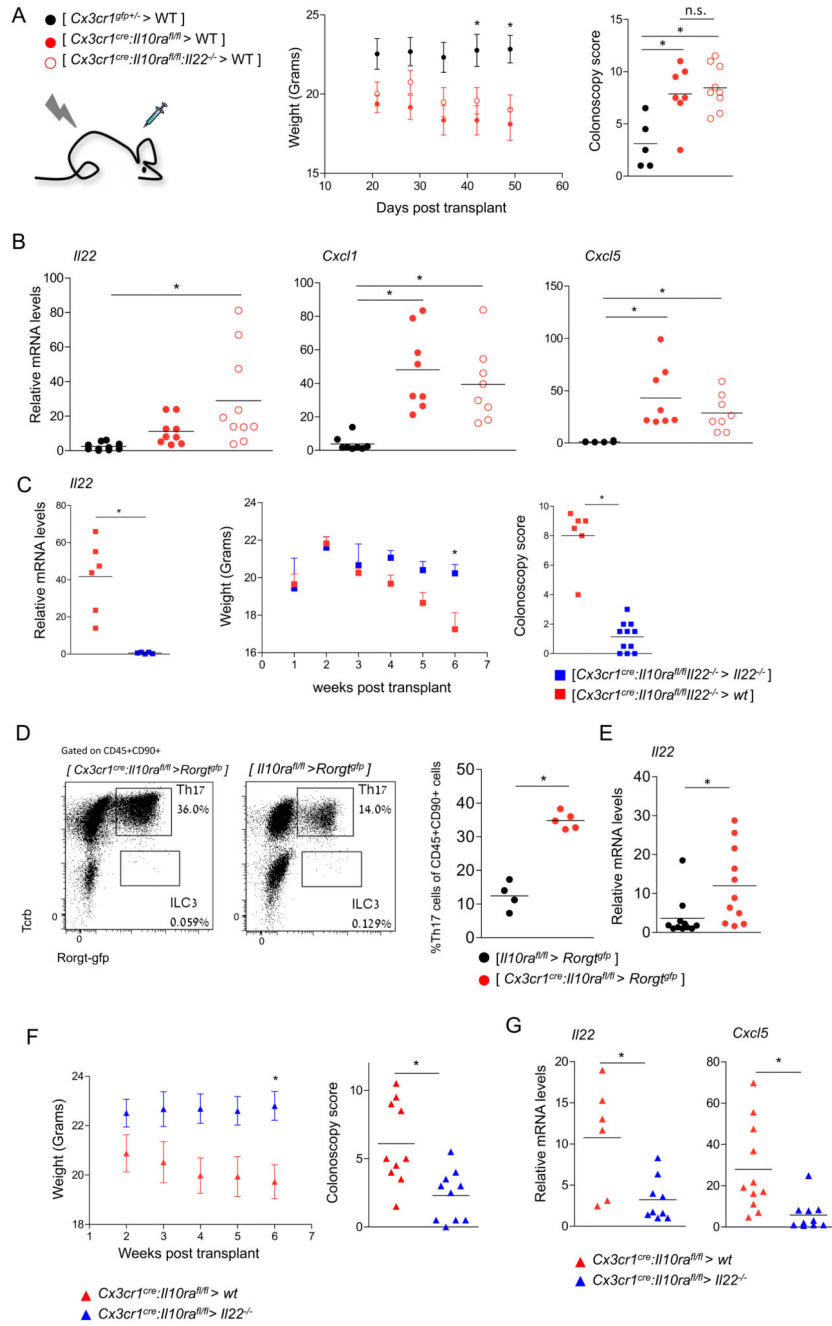
Figure 5. Definition of the cellular source of IL-22.

(**A**) Weight and colonoscopic analysis of *[Cx3cr1^{cre}:Il10ra^{fl/fl} > WT]*, *[Cx3cr1^{gfp/+} > WT]* or *[Cx3cr1^{cre}:Il10ra^{fl/fl}:Il-22^{-/-} > WT]* BM chimeras. Colonoscopy was performed 6 weeks post-transplant. Data are collected from 2 independent experiments, n>=3 in each.

(**B**) qRT-PCR analysis of *il22*, *cxcl1* and *cxcl5* expression in whole tissue extracts of colons of indicated BM chimeric mice. Data are collected from 2 independent experiments, n=3-5 in each group.

(C) qRT-PCR analysis of il22 expression in whole tissue extracts of colons of indicated BM chimeric mice. Data are from one representative experiment of two. (left)

Weight and colonoscopic analysis of [*Cx3cr1^{cre}:Il10ra$^{fl/fl}$:Il22$^{-/-}$* > WT], [*Cx3cr1^{cre}:Il10ra$^{fl/fl}$:Il22$^{-/-}$* > *Il22$^{-/-}$*] BM chimeras. Colonoscopy was performed 7 weeks post-transplant. Weight data are from one representative experiment of two, n=3-4 in each group, colonoscopy data are collected from two experiments, n=3-4 in each. (right)

(D) Flow cytometry analysis of the *lamina propria* of [*Cx3cr1^{cre}:Il10ra$^{fl/fl}$* > *Rorgt^{gfp}*], [*Il10ra$^{fl/fl}$* > *Rorgt^{gfp}*] BM chimeras. Data are representative of three experiments, n=3-5 in each group.

(E) qRT-PCR analysis of *il22* expression by sorted Th17 cells from indicated BM chimeras. Data are collected from three independent experiments, n=3-5 in each group.

(F) Weight and colonoscopic analysis of [*Cx3cr1^{cre}:Il10ra$^{fl/fl}$* > WT] or [*Cx3cr1^{cre}:Il10ra$^{fl/fl}$* > *Il- 22$^{-/-}$*] BM chimeras. Colonoscopy was performed 6 weeks post-transplant. Data are collected from 2 independent experiments, n>=3 in each**.**

(G) qRT-PCR analysis of *il22* and *cxcl5* expression in whole tissue extracts of colons of indicated BM chimeric mice. Data are collected from 2 independent experiments, n=3-5 in each group.
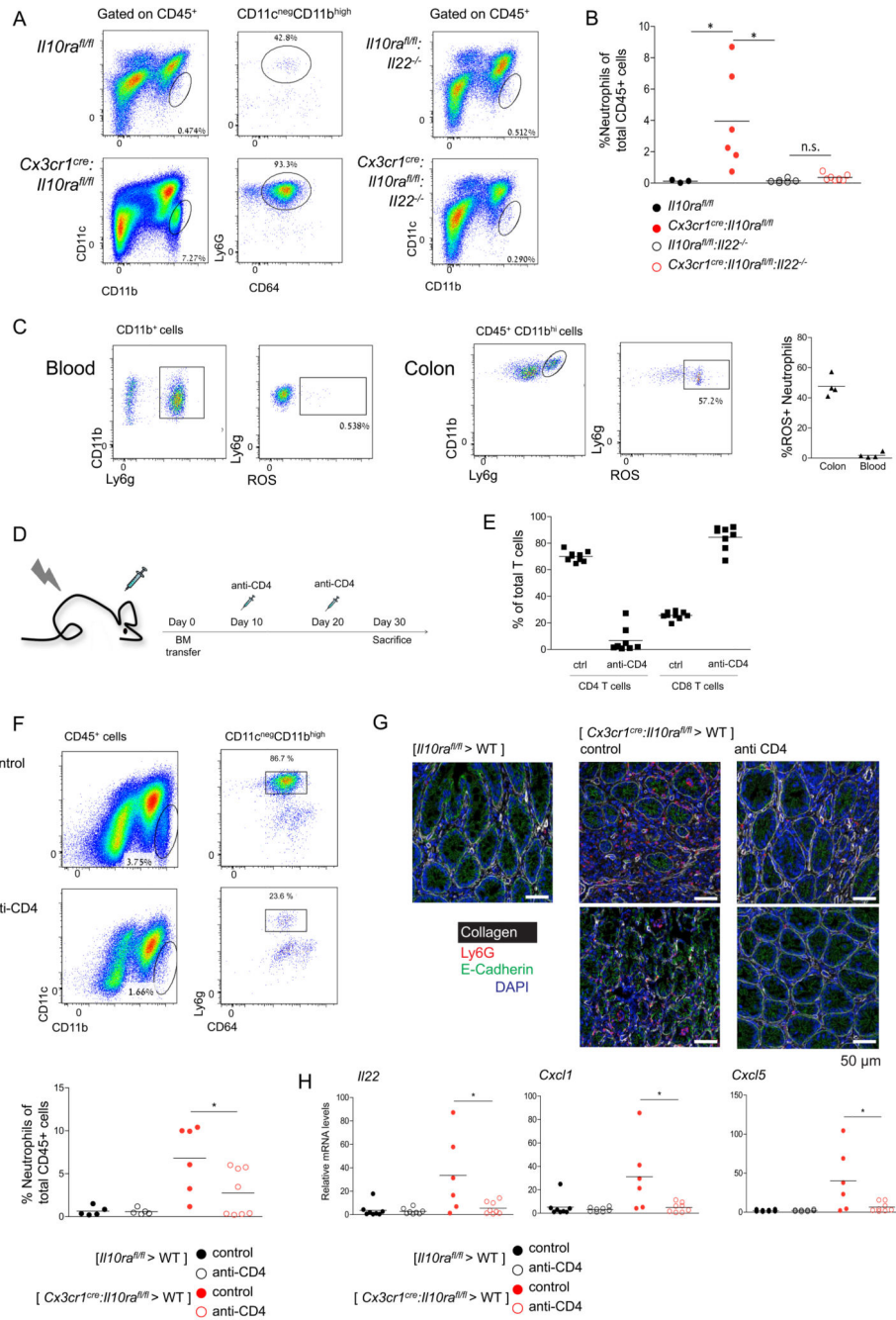
Figure 6. Neutrophil recruitment to the colonic *lamina propria* depends on CD4+ T cells.
(A) Representative plots of flow cytometry analysis of the colonic *lamina propria* of indicated mouse strains.

(B) Quantification of flow cytometry analysis according to gating strategy indicated in A.

(C) Representative plots of flow cytometry analysis of the colonic *lamina propria* of *Cx3cr1*^cre^*:Il10ra*^fl/fl^ mice (left). Quantification of flow cytometry analysis (right).

(D) Schematic of T cell depletion protocol

(E) Quantification of flow cytometry analysis of mesenteric LN indicating efficient ablation of CD4$^+$ T cells, but not CD8$^+$ T cells.

(F) Representative plots of flow cytometry analysis of the colonic *lamina propria* of [*Cx3cr1^{cre}:Il10ra$^{fl/fl}$* > WT] BM chimeras.

(G) Representative immunofluorescence images of colon sections of [*Il10ra$^{fl/fl}$* > WT] BM chimeras, [*Cx3cr1^{cre}:Il10ra$^{fl/fl}$* > WT] BM chimeras and [*Cx3cr1^{cre}:Il10ra$^{fl/fl}$* > WT] BM chimeras treated with the anti-CD4 regimen.

(H) qRT-PCR analysis of *il22*, *cxcl1* and *cxcl5* expression in whole tissue extracts of colons of indicated BM chimeric mice.

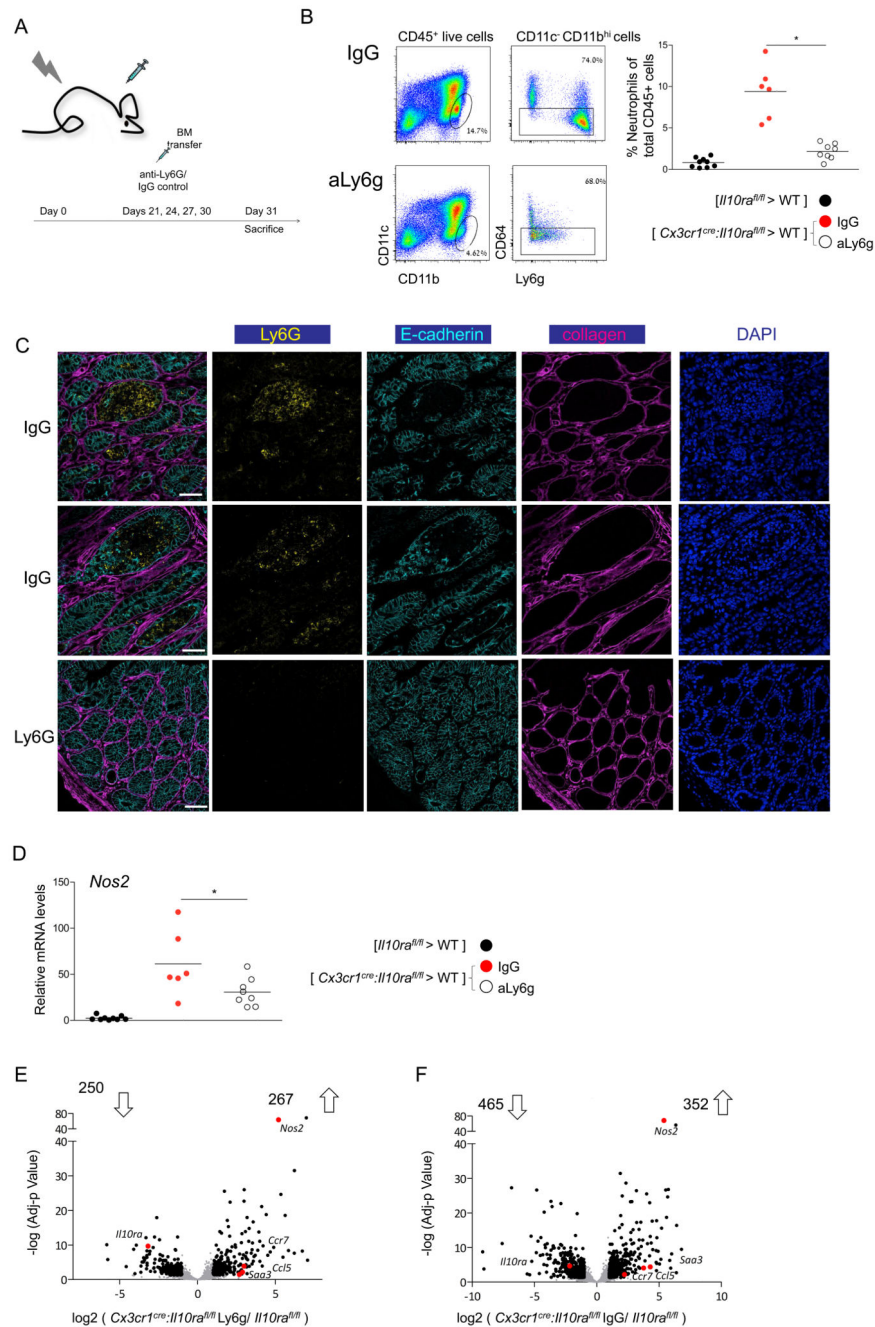Data are collected from two independent experiments, n>=3 in each

Figure 7. Neutrophil depletion ameliorates colitis in *Cx3cr1^cre^:Il10ra^fl/fl^* BM chimeras

(**A**) Schematic of neutrophil depletion protocol

(**B**) Representative plots of flow cytometry analysis of the colonic *lamina propria* of
[*Cx3cr1^cre^:Il10ra^fl/fl^* > WT] BM chimeras treated with IgG control or anti Ly6G antibody
(left). Quantification of flow cytometry analysis (right).

(**C**) Representative immunofluorescence images of the colonic tissue of
[*Cx3cr1^cre^:Il10ra^fl/fl^* > WT] BM chimeras treated with IgG control or anti Ly6G antibody**.**

(D) qRT-PCR analysis of *Nos2* expression in whole tissue extracts of colons of indicated BM chimeric mice.

(E-F) Volcano plot of statistical significance (log10 p-value) against log 2 ratio of macrophages isolated from colonic tissue of [*Cx3cr1*^{cre}:*Il10ra*^{fl/fl} > WT] BM chimeras treated with IgG control

(F) or anti Ly6G antibody (E) and [*Il10ra*^{fl/fl} > WT] BM chimeras, based on RNA-seq data. Significantly up or down regulated genes (fold change>2, adj-p value<0.05) are in black, relevant pro inflammatory up-regulated genes are highlighted in red.

Data in A-D are collected from two independent experiments, n>=3 in each